Effect of diamagnetic doping on the magnetic resonance in a quasi-one-dimensional system tetramethylammonium manganese trichloride

L. Allam, G. Ablart, and J. Pescia
Laboratoire de Magnétisme et d'Electronique Quantique, Université Paul Sabatier, 118 route de Narbonne, 31062 Toulouse CEDEX, France

S. Clément and J. P. Renard
Institut d'Electronique Fondamentale Bâtiment 220, Université de Paris XI, 91405 Orsay CEDEX, France
(Received 25 July 1988; revised manuscript received 26 May 1989)

We present electron-spin-resonance data obtained on finite magnetic chains of $CH_3NMn_{1-x}Cd_xCl_3$ (TMMC-Cd) for $x=0.02$, 0.09, and 0.2. The measurements were developed with the microwave field either parallel or perpendicular to the magnetic field. The longitudinal relaxation time was also measured in the $x=0.02$ and 0.09 samples. All our experimental results show a noticeable influence of the impurities on both the line shape and linewidth, contrary to previously published data. New nuclear magnetic resonance data dealing with high-frequency proton relaxation rates are also presented. A full treatment using the memory-function formalism has been carried out to account for the significant difference observed between pure and doped samples. Our experimental data are satisfactorily described by this theory and the model of correlation functions for finite chains.

I. INTRODUCTION

During the past yen years, one-dimensional (1D) magnetic materials have been thoroughly investigated. In particular, the spin dynamics at high temperature has been studied by magnetic resonance techniques.[1] Measurement of the nuclear relaxation times has given information on the coupling between the nuclei and the paramagnetic ions. These times are related to two-spin time correlation functions or, more precisely, to their Fourier transforms or "spectral densities" at the electron (nuclear) angular frequencies $\omega_e(\omega_n)$. On the other hand, electron spin resonance (ESR) may give information about a special function $\phi(t)$ which is composed of four-spin correlation functions. The aforesaid functions are characterized at long times by a diffusive process: They decrease slowly following a $(Dt)^{-1/2}$ law (D being a spin-diffusion coefficient), and finally they cancel at a cutoff time owing to anisotropic or interchain interactions. Such properties have been observed experimentally in several quasi-1D systems and principally in tetramethylammonium trichloromanganate $(CH_3)_4NMnCl_3$ (TMMC) which is the real system the nearest to the theoretical 1D model.[1]

Interesting results have also been obtained in doped systems. Replacing Mn^{2+} ions by Cu^{2+} in TMMC, an appreciable broadening of the ESR line[2] and a shortening of proton relaxation time[3] are found. These effects are explained by a slowing down of the diffusion rate along the linear chains, due to Cu^{2+} impurities. Let x be the impurity concentration; the resulting spin-diffusion coefficient $D(x)$ can be evaluated using a model proposed by Richards.[2] Stronger effects are observed in 1D systems doped by diamagnetic impurities. Here, the impurities behave like quasiperfect reflectors for the spin polarization. Proton relaxation rate is enhanced by a factor as high as 30 in TMMC doped with 20 at. % Cd.[4] This should be compared to the TMMC-Cu case where this ratio is only 3 with the same impurity concentration. However, in ESR experiment, the situation is more complicated than in NMR. An increase of the ESR linewidth with a weakly doped sample was first observed by Clément *et al.*[3] and this result was confirmed with more doped samples by the authors.[5] Recently, Karra *et al.*[6,7] have reported very different experimental data. According to them, doping does not significantly modify the linewidth but only alterates the line shape far in the wings. Moreover, the occurrence of hyperfine structure, usually encountered in isolated paramagnetic ions, is reported in the heavily doped samples. Since the doping in 1D compounds usually increases the linewidth (except in some pathological cases), the results of Karra *et al.* are highly surprising and need to be clarified.

In this article, we present an analysis of ESR experiments on TMMC samples doped with different Cd^{2+} ion concentrations $x=0.02$, 0.09, and 0.20. We have measured at room temperature and at X-band the derivated absorption spectra as a function of θ, the angle between the magnetic field $\mathbf{H}_0$ and the $\mathbf{c}$ chain axis. Two configurations of the oscillating field $\mathbf{H}_1$ have been considered: the usual resonance configuration (where the fields are perpendicular) and the relaxation configuration (where the fields are parallel). We have also measured the electron longitudinal relaxation rate using the modulation method. We present furthermore new NMR data dealing with high-frequency proton relaxation rates. Special attention is paid to the orientation $\theta\approx 0°$ where spin diffusion is expected.

In Sec. II, we describe the sample preparation and the apparatus used. Our experimental data are reported in Sec. III, showing unambiguously the doping influence on the ESR spectra. An attempt for explaining the negative

results of Karra is proposed. The linewidths and the line shifts need to take into account many terms which are usually neglected. The complete theory is presented in Sec. IV within the memory-function formalism. Experimental results are interpreted in Sec. V using this theory and the correlation function model for the finite chains. The conclusions are presented in Sec. VI.

II. THE SAMPLES AND THE APPARATUS

The $(CH_3)_4NMn_{1-x}Cd_xCl_3$ single crystals have been grown by slow evaporation at 30 °C of saturated solution of $(CH_3)_4NCl$ and $x CdCl_2 2H_2O + (1-x)MnCl_2 4H_2O$ in $2N$ HCl. The crystals so obtained are whitish and must be kept from altering by moisture. The Mn (TMMC) and Cd (TMCC) pure salts have similar crystallographic structures.[8,9] In TMMC:Cd, the Cd-Cd separation is of 3.36 Å inside a chain and of 9.13 Å between chains while in TMMC, the Mn-Mn separation values are, respectively, 3.25 and 9.15 Å. It is expected that in the doped samples the Cd ion takes the place of the Mn one.

The linewidth and line shift have been measured using an X-band homodyne spectrometer operating at room temperature. T_{1e} measurements were also performed at X-band, by means of a "modulation spectrometer," a detailed description of which has already been given elsewhere.[10,11] The microwave field is amplitude modulated at the angular frequency Ω. The signal at resonance is induced in a pickup coil placed close to the sample and along the magnetic field. When $\Omega T_{1e} \ll 1$, the longitudinal magnetization follows the law of induction and the signal S is proportional to Ω. When $\Omega T_{1e} \gg 1$, the signal tends towards a limiting value S_0. T_{1e} can be determined from the curve $S(\Omega)$. For very short times ($T_{1e} < 10^{-8}$ s) S_0 is obtained by comparison with a test sample.[12]

The proton relaxation time T_{1n} was measured by means of spectrometer Brüker SXP in the frequency range 10–72 MHz. The conventional $\Pi - \Pi/2$ pulse method was used. Generally, the recovery of nuclear magnetization was not exponential. T_{1n} was defined as the time required for the off-equilibrium signal to fall to e^{-1} of its initial amplitude.

III. EXPERIMENTAL RESULTS

A. ESR with resonance configuration

The spectrum observed in this configuration reveals different compounds. An example is given in Fig. 1, showing the derivative absorption in the most doped sample ($x = 0.20$) when the static field is parallel to the chain axis. Three kinds of lines can be seen:

(i) A relatively narrow, central line which is produced by isolated Mn^{2+} ions. It corresponds indeed to the one which was observed in pure TMMC at low temperatures,[13] and attributed to the same causes.[5]

(ii) A symmetrical structure (ten lines) resulting from ions pairs. Such a structure appears also, though faintly, in a sample with lower impurity concentration ($x = 0.09$). These dimmer lines broaden and disappear when the angle between the chain axis and the Zeeman magnetic field

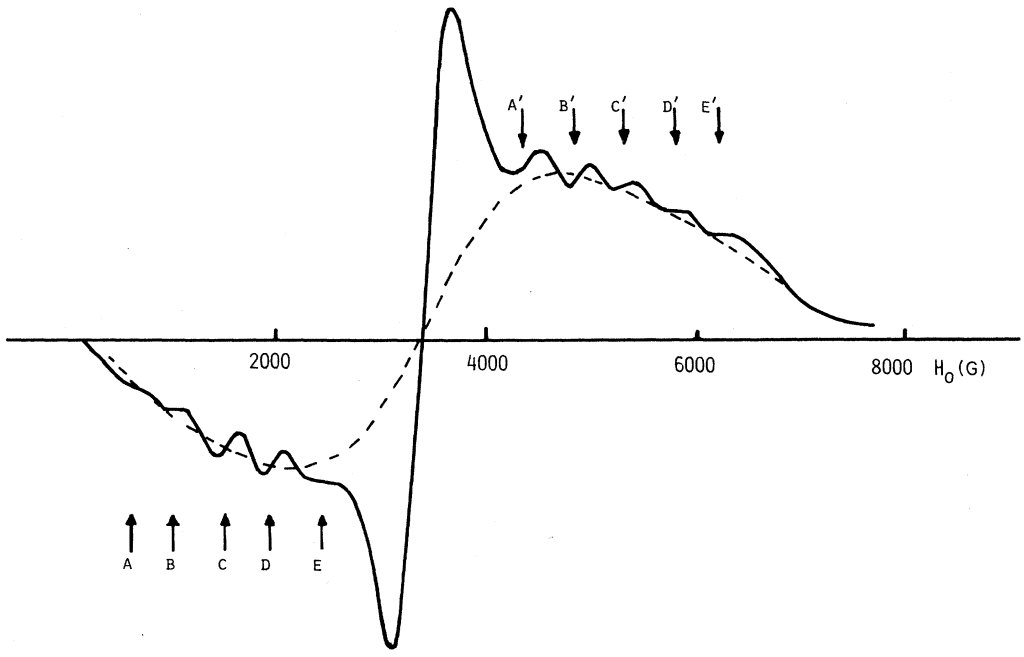

FIG. 1. ESR spectrum at room temperature for TMMC doped with Cd ($x = 0.20$). The magnetic field is parallel to the chain axis.

H_0 exceeds 20°. It was studied in a separate publication.[5]

(iii) The broad line on which are superimposed the preceding ones is attributed to the Mn^{2+} belonging to finite chains bounded by diamagnetic impurities. The observation of pairs of Mn^{2+} ions gives clear evidence that diamagnetic Cd^{2+} ions really entered into the TMMC matrix. On Figs. 2 and 3 are plotted room-temperature data concerning linewidths and line shifts, respectively, of pure and doped TMMC versus orientation; Cd concentrations are $x=0$ for pure TMMC and $x=0.02$, 0.09, and 0.2. Large enhancements of linewidths and line shifts by the doping are observed. As an example, in the sample doped with $x=0.20$, the static field being directed along the chain axis, the linewidth is more than three times the one in pure TMMC. A line-shape analysis is difficult, owing to the structure aforementioned.

Our results are in strong disagreement with those reported by Karra *et al.*[6,7] These authors reported that the linewidths and line shifts were not changed by the doping but fine and hyperfine structures appeared in the most doped samples. A slight change from 1D character of the line shape was only found. We think that the trouble arises in fact from the quality of the crystals used by these authors. As it was noted by Dupas and Renard,[14] good quality crystals of TMMC:Cd are exceedingly difficult to grow. The essential reason is that the impurity concentration x is 50 times larger than the cadmium concentration of the starting solution. It results that an homogeneous impurity distribution of Cd ions in the crystal is difficult to realize. The fine and hyperfine structure reported by Karra *et al.* coincide with those found by McPherson *et al.* and by Tazuke[15] in the cadmium matrix (TMCC) doped by a low concentration of Mn^{2+} ions. This suggests that the crystals used by Karra *et al.* may be composed of very weakly doped TMCC and TMMC phases.

B. ESR with relaxation configuration

In this configuration the oscillating field (at angular frequency ω) is linearly polarized in a direction parallel to the static field. Measurement of the ESR linewidths in

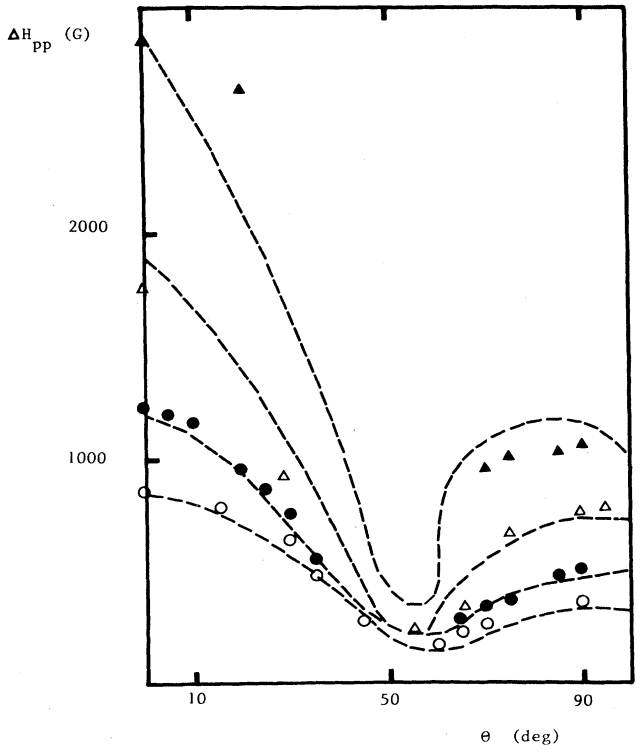

FIG. 2. Angular variation of the peak-to-peak ESR linewidth in TMMC:Cd at 300 K and 9 GHz in the resonance configuration. The measurements have been performed using a conventional homodyne spectrometer. θ is the angle between the magnetic field and the chain axis. Impurity concentrations are $x=0$ (○), $x=0.02$ (●), $x=0.09$ (△), and $x=0.2$ (▲).

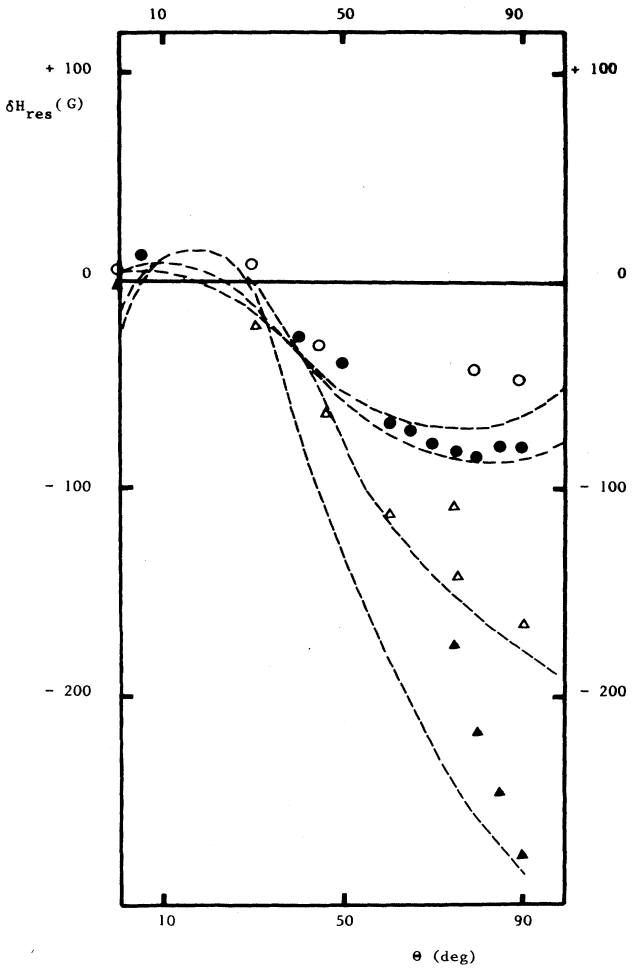

FIG. 3. Angular variation of the ESR line shift in TMMC:Cd at 300 K and 9 GHz in the resonance configuration. The measurements have been performed using a conventional homodyne spectrometer. θ is the angle between the magnetic field and the chain axis. Impurity concentrations are $x=0$ (○), $x=0.02$ (●), $x=0.09$ (△), and $x=0.2$ (▲).

the relaxation configuration is unusual because it is difficult to set up. However it is interesting because it characterizes specifically the samples, the memory functions being approximately described by the line shapes. Furthermore, the lines resulting from single or paired Mn^{2+} ions disappear, leaving only pure one-dimensional effects. Earlier measurements were done on pure TMMC by Lagendijk and Schoemaker,[16] showing a characteristic line at half-field resonance. A predicted line at the normal resonance field was hidden by the strongly allowed transition of the resonance configuration. Here, we were able to observe these two lines, owing to the well-defined polarization of the microwave field. Examples of recorded lines obtained in doped TMMC ($x=0.2$) are presented in Fig. 4. Both lines disappear near $\theta=0°$, while the high-field line vanishes for $\theta=90°$. Line broadening and large line shifts (up to 2000 G!) are observed in this doped sample. The resonance field and the peak-to-peak linewidths have been plotted on Figs. 5 and 6 for both lines versus the angle θ.

C. Electron spin-lattice relaxation time

The evolution of the electron relaxation rate T_{1e}^{-1} for pure and doped TMMC versus θ, the angle between the resonance field H_0 and the chain axis, is presented in Fig. 7. Measurements have been carried out for 2 and 9 at. % only. In effect, for 20 at. % Cd the broadening of the line prevents relaxation rate measurement. The reduction of the relaxation rate by doping is clearly seen in Fig. 7.

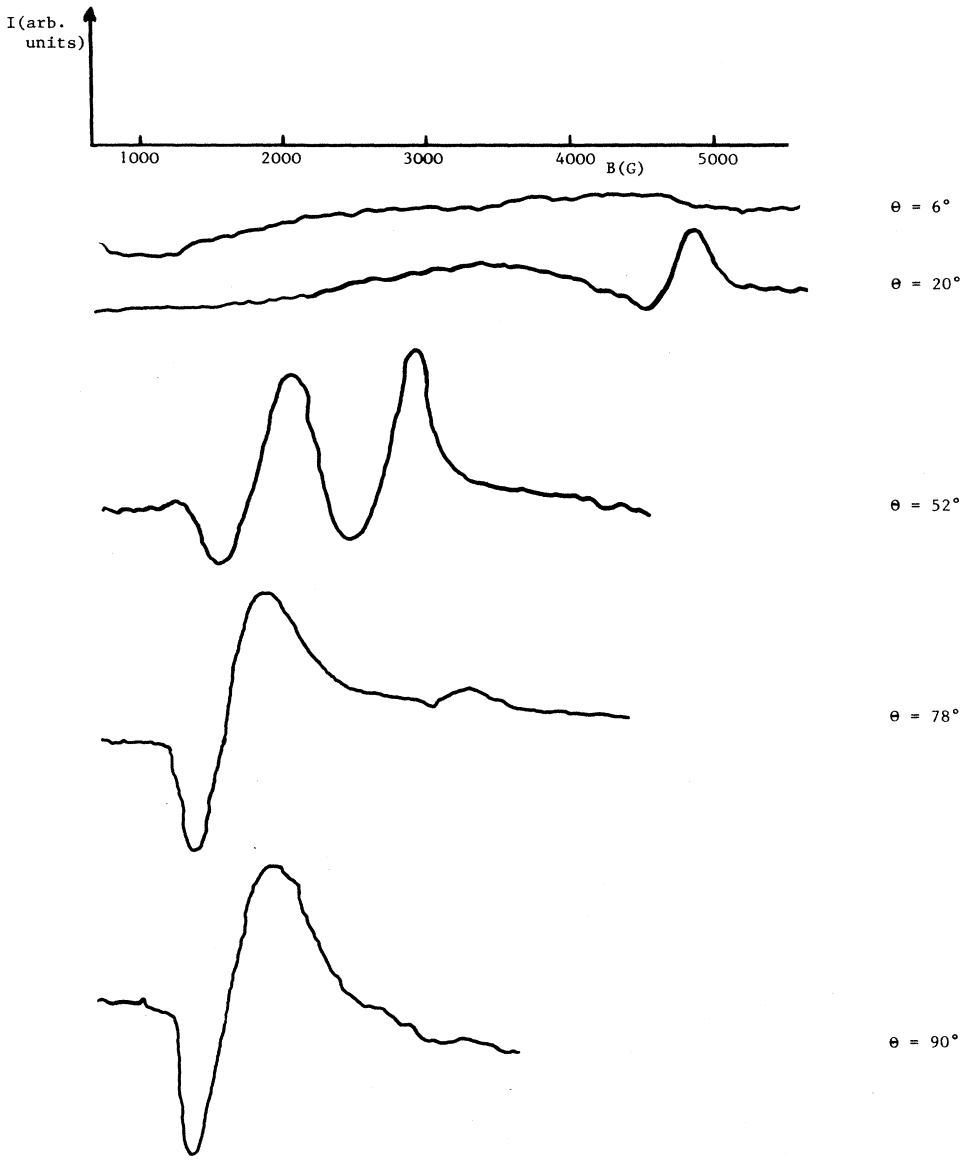

FIG. 4. Angular variation of the field resonance of the two lines in the relaxation configuration.

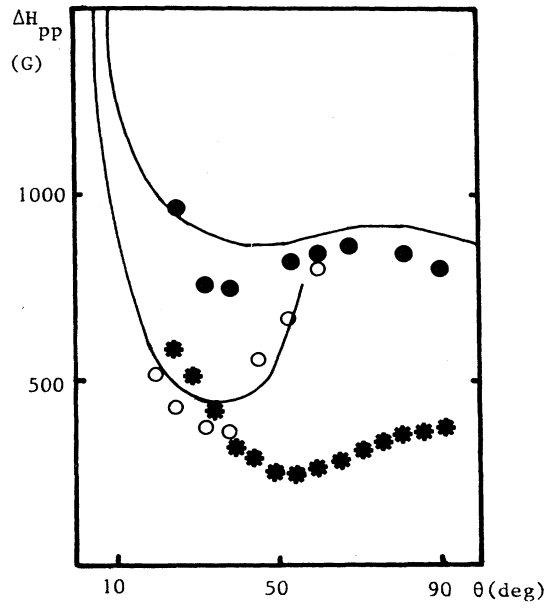

FIG. 5. Angular dependence of the peak-to-peak ESR linewidth in TMMC:Cd ($x=0.20$) at 300 K and 9 GHz in the relaxation configuration at half (●) and normal resonance field (○). Lagendijk and Schoemaker results (*). The solid line corresponds to theory.

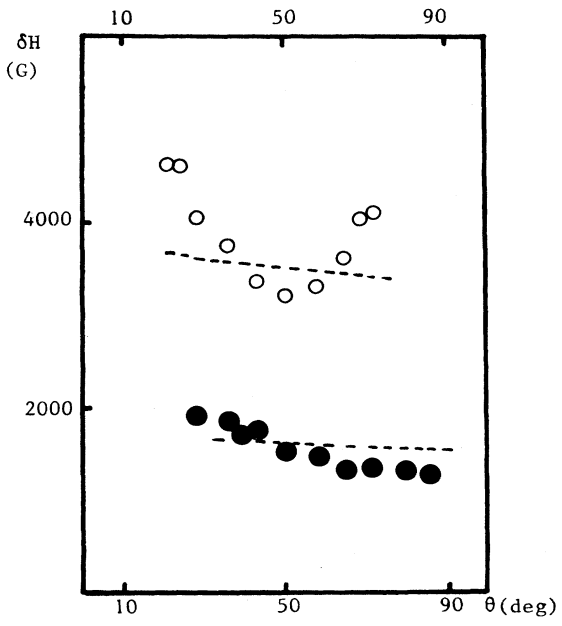

FIG. 6. Angular dependence of the line shift in TMMC:Cd ($x=0.20$) at 300 K and 9 GHz in the relaxation configuration at half (●) and normal resonance field (○). Dashed line: theory.

This behavior is apparently surprising, but it was previously expected from proton relaxation rates measurement.[4]

D. Proton spin-lattice relaxation time T_{1n}

The doping strongly shortens the proton spin-lattice relaxation time T_{1n}.[4] Here we have studied the frequency dependence of T_{1n}, which gives information on the spectral densities of electron spins. The evolution of the proton spin-lattice relaxation time T_{1n} versus θ in doped ($x=0.20$) TMMC is presented in Fig. 8 for various nuclear frequencies ν_n. When the frequency is raised an important lengthening of T_{1n} is observed at low values of θ, but this lengthening is very weak for $\theta>50°$. Such a behavior is also observed in less doped samples ($x=0.09$ and 0.02) but with longer times. In all samples the results for $\theta=0°$ and $\theta=10°$ can be fitted with the relation

$$T_{1n}^{-1}(x)=P(x)(\nu_n)^{-1/2}+Q(x)\ , \tag{1}$$

showing the existence of a diffusion process as in pure TMMC (Fig. 9). The value of $P(x)$ increases strongly with the doping, while $Q(x)$, which is positive for $x=0$, decreases and becomes negative in doped samples.

IV. GENERAL THEORY

A. ESR calculation

The influence of doping on the ESR linewidth in 1D chains has been studied by several authors.[2,17] The main mechanism for the broadening of the ESR line is the dipolar interaction between spins belonging to the same chain. The presence of a strong exchange interaction along the chain axis leads to the diffusion of magnetization. To interpret our results which are characterized by a large broadening of the line, out of the usual ESR conditions (i.e., $\Delta H_{pp}\ll H_0$), it is necessary to use a calculation valid for the whole rangle of frequencies and magnetic resonance fields. This calculation has been developed previously,[18,19] and only the main results are recalled here. In the usual configuration of fields (the static field and the oscillating field being perpendicular) the absorption spectrum can be written as

$$I(\omega)\sim \mathrm{Re}[a^{zz}(a^{2+}+a^{2-}+a^{+-}+a^{-+}) +(a^{z-}-a^{z+})(a^{-z}-a^{+z})]/D\ , \tag{2}$$

with

$$D=(a^{+-}a^{-+}a^{zz}-a^{+-}a^{-z}a^{z+}-a^{zz}a^{2+}a^{2-} -a^{2+}a^{-z}a^{z-}-a^{-+}a^{z-}a^{+z})\ .$$

The $a^{\alpha\beta}$ terms calculated for a linear chain of spins coupled by exchange and dipolar interactions are given in the Appendix with some other details. In the mathematic expressions appear functions $\tilde{\Phi}(\omega,\omega_z)$ which are related to the dynamic behavior of four-spin correlations, for an applied static field ω_2 (in angular frequency unit).

The relation (2) yields the correct description whenever the linewidth (in angular frequency unit) is comparable to

ω and ω_z.[18] At high frequency/field the terms a^{+-} and a^{zz} are dominant and one recovers the usual relation[1]

$$I(\omega) \propto \mathrm{Re}[i(\omega-\omega_z)+\tilde{K}_{-+}(\omega)]^{-1} ,$$

$\tilde{K}_{-+}(\omega)$ being a memory function.

For the relaxation configuration one gets then

$$I_z(\omega)=\langle S^z S^z\rangle (a^{+-}a^{-+}-a^{2+}a^{2-})/D \qquad (3)$$

where $I_z(\omega)$ is proportional to the line absorption in this configuration.

For $\theta=90°$ one has simply

$$I_z=\langle S^z S^z\rangle (a^{zz})^{-1} .$$

When a strong exchange is present, the electron spin-lattice relaxation rate is usually depicted by the three-reservoirs model of Bloembergen and Wang.[20] In TMMC at room temperature the spin-lattice relaxation time T_{1e} can be calculated by the Kubo-Tomita[21] approach.

$$T_{1e}^{-1} \sim \{\sin^2\theta\cos^2\theta[\tilde{\Phi}(\omega_z)+\tilde{\Phi}(-\omega_z)] + \sin^4\theta[\tilde{\Phi}(2\omega_z)+\tilde{\Phi}(-2\omega_z)]\} .$$

B. NMR calculation

The relaxation rate of protons comes essentially from the fluctuations of the dipolar interaction which couples

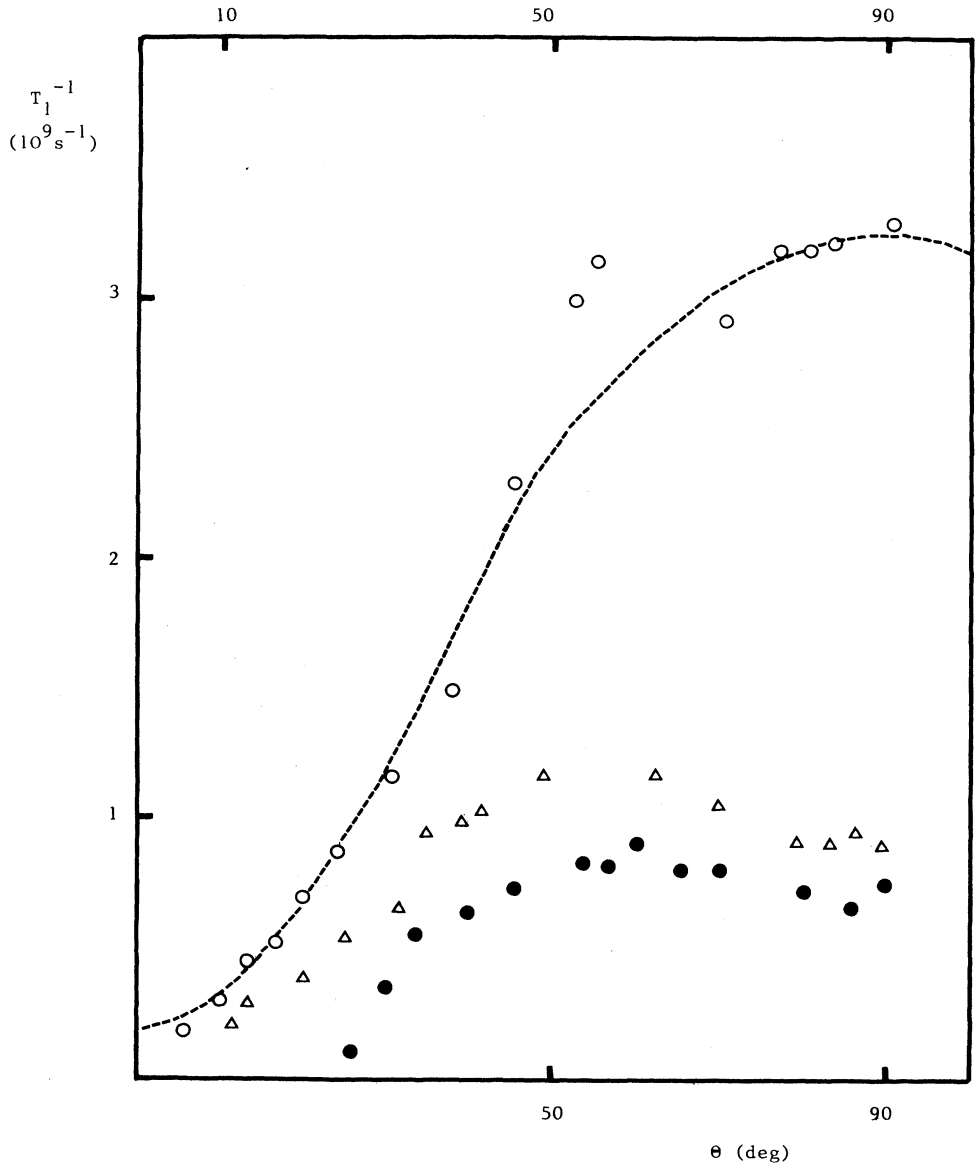

FIG. 7. Angular variation of the spin-lattice relaxation rate in TMMC:Cd at 300 K and 9 GHz. The measurements have been performed with a "modulation" spectrometer. Impurity concentrations are $x=0$ (○), $x=0.02$ (●), and $x=0.09$ (△). Dashed line: theory.

them with the Mn^{2+} electron spins. For one-dimensional systems one can write[1]

$$T_{1n}^{-1}=(\tfrac{2}{3})S(S+1)\sum_j A_j f_j^z(\omega_n)+B_j f^+ j(\omega_e) .$$

$f_j^\alpha(\omega)$ are the Fourier transforms of the spin-correlation functions

$$g_j^\alpha(t)=[S(S+1)]^{-1}\langle S_i^\alpha(t)S_{i+j}^{\alpha *}(0)\rangle .$$

Here S_{i+j}^α is the α (z or $+$) spin component of the jth neighbor of the spin $\mathbf{S}_i$ at site i. The A_j and B_j terms are geometric coefficients which depend on the angle θ. The positions of protons in TMMC are not exactly known but A_j and B_j can nevertheless be evaluated by using various models of location.

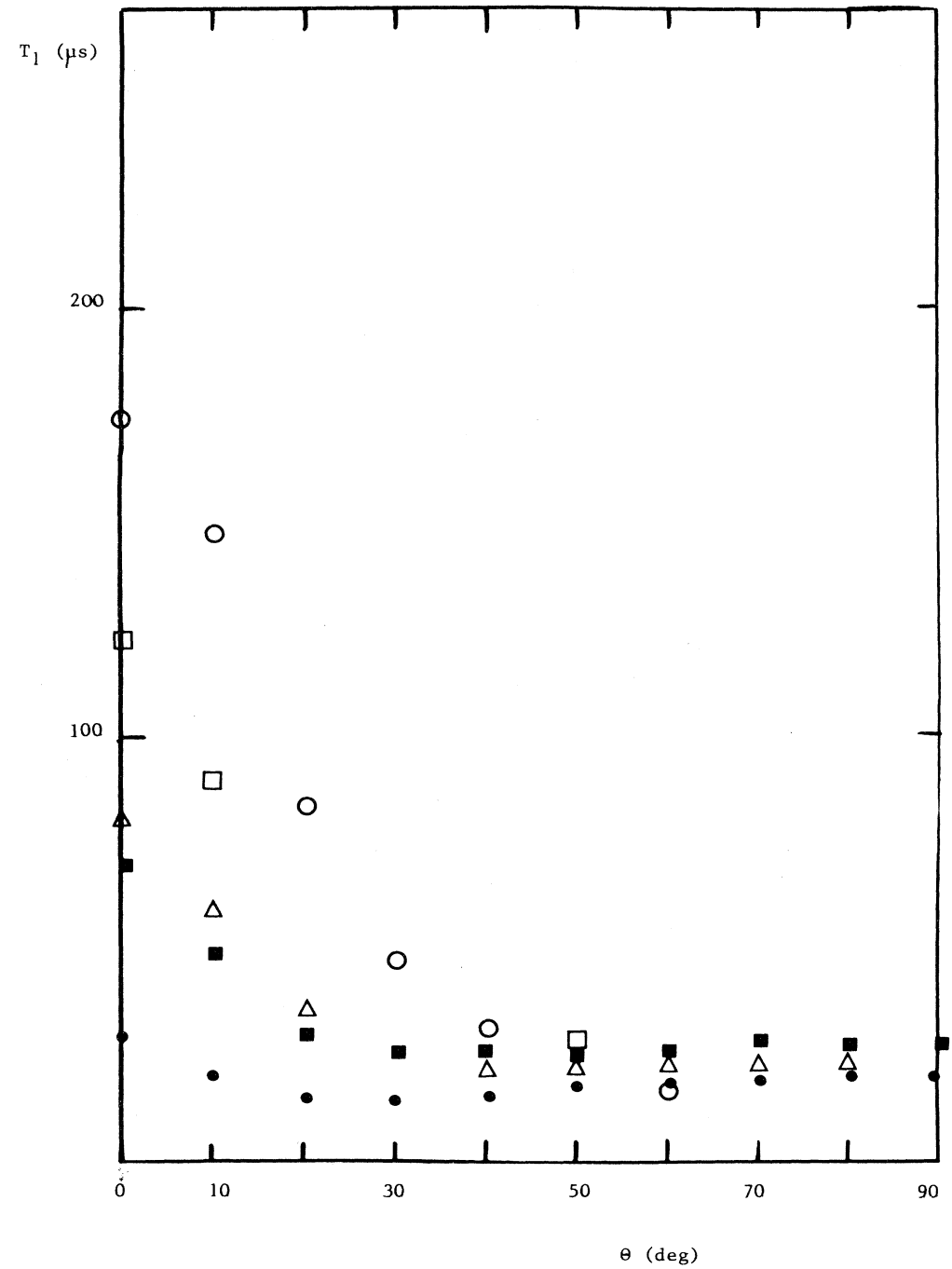

FIG. 8. Angular dependence of the proton spin-lattice relaxation time T_{1n} for several frequencies at 300 K in TMMC doped with Cd: ○, 72 MHz; □, 54.3 MHz; △, 40.2 MHz; ■, 27.1 MHz; ●, 14 MHz.

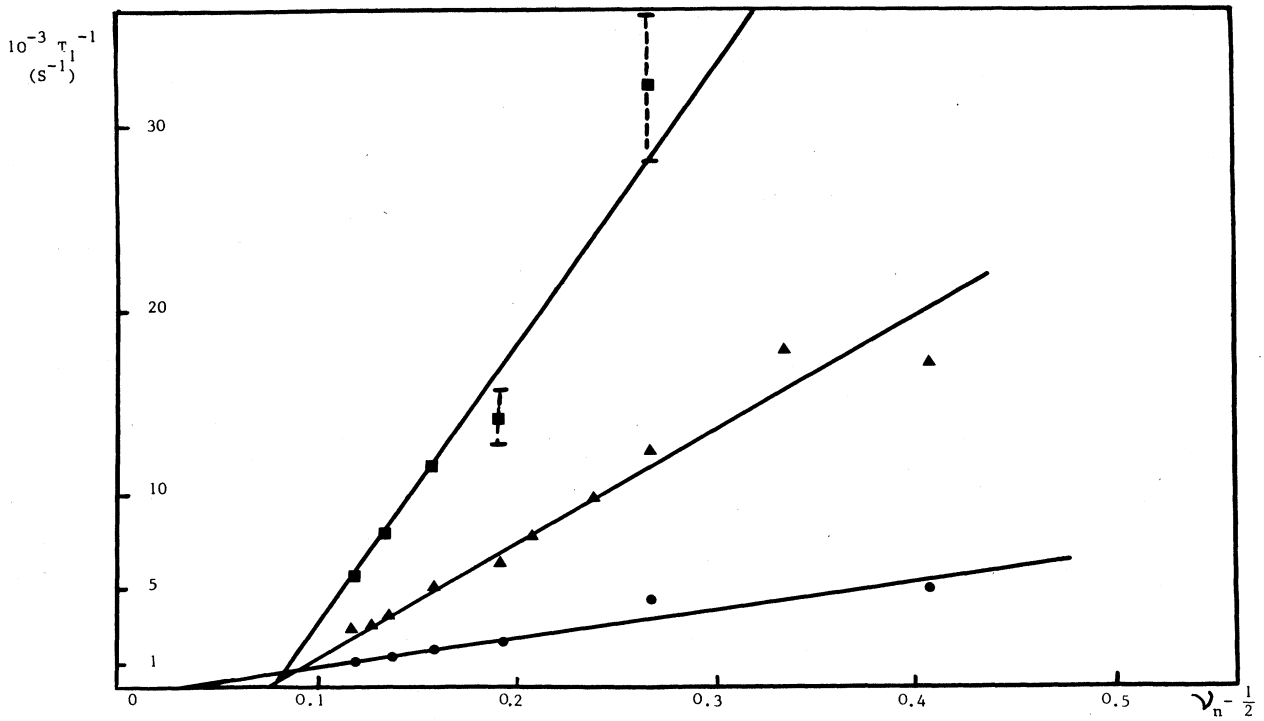

FIG. 9. T_{1n}^{-1} variation vs $\nu_n^{-1/2}$ for $\theta=0°$ in doped TMMC samples (▲, $x=0.09$; ■, $x=0.20$). The straight lines give the P and Q values.

V. INTERPRETATION AND DISCUSSION OF EXPERIMENTAL RESULTS

A. The spin dynamics model

In pure 1D systems the correlation functions $g(t)$ or $\phi(t)$, after an initial Gaussian decay, become diffusive at a "diffusion time" t_D, and finally cancel at a cutoff time t_c. One has $D\sim\omega_{ex}$, the exchange frequency, and $t_D\gg\omega_{ex}^{-1}$. In our case the same dipolar interactions are responsible for the cutoff mechanism and the ESR linewidth ΔH so that $t_c^{-1}=\omega_c\sim\gamma_e\Delta H$.

In paramagnetically doped compounds the enhancement of the relaxation rates is explained by the reduction of the spin-diffusion coefficient D. In addition to the diffusion slowing down there is an increase of t_D.

In diamagnetically doped samples (TMMC-Cd), a linear chain of spins is broken into quasinoninteracting segments. We can consider as an approximation a n-spins finite chain. Computer simulations on classic spins[22] show that correlation functions rapidly attain a constant value if n is not too high ($n\leq 10$). Spin diffusion, if any, is insured by the weak interaction between Mn spins separated by Cd atoms and thus occurs at very long times t_D. As a result the diffusion coefficient is extremely small, but the diffusion regime lasts a relatively short time, beginning at a longer time t_D and ending at a shorter t_c, since the linewidth is broadened (Fig. 10). It follows that the frequency spectrum becomes strongly peaked at very low frequencies ($\omega=0$, ω_n) while it is depressed at intermediate frequencies (ω_e).

B. Analysis of the NMR results

The NMR results are somewhat easier to analyze and we consider them first. We discuss here essentially the new results concerning the frequency dependence near $\theta=0°$. The results for $\theta\geq 50°$ were explained in a previous paper[23] and it was shown that necessarily the cutoff ω_c^z, and thus T_{1e}^{-1}, should be reduced by the doping. This is indeed experimentally verified (Fig. 7).

We proceed now to the spin dynamics model mentioned in the preceding section. The limit of the two-spin correlation functions g_j ($t\to\infty$) is approximately n^{-1} if exchange interactions only are involved. Here we neglect the boundary effects occurring for the shorter chains. We define the following model for an n-spins chain:

$$0\leq t\leq t_D,\quad g_j(t)=g(t)=n^{-1};$$

$$t_D\leq t<\infty,\quad g(t)=[2\Pi D(x)t]^{-1/2}e^{-\omega_c(x)t}.$$

$D(x)$ is an "averaged" diffusion coefficient, which is a decreasing function of the concentration x. The Fourier transform of $g(t)$ at frequency $\omega\ll\omega_c$ is

$$\tilde{f}(\omega)=G-n[2\Pi D(x)]^{-1}+[D(x)\omega_c]^{-1/2}. \quad (4)$$

The diffusion can be observed with the condition $t_D^{-1}\gg\omega\gg\omega_c$. In this case

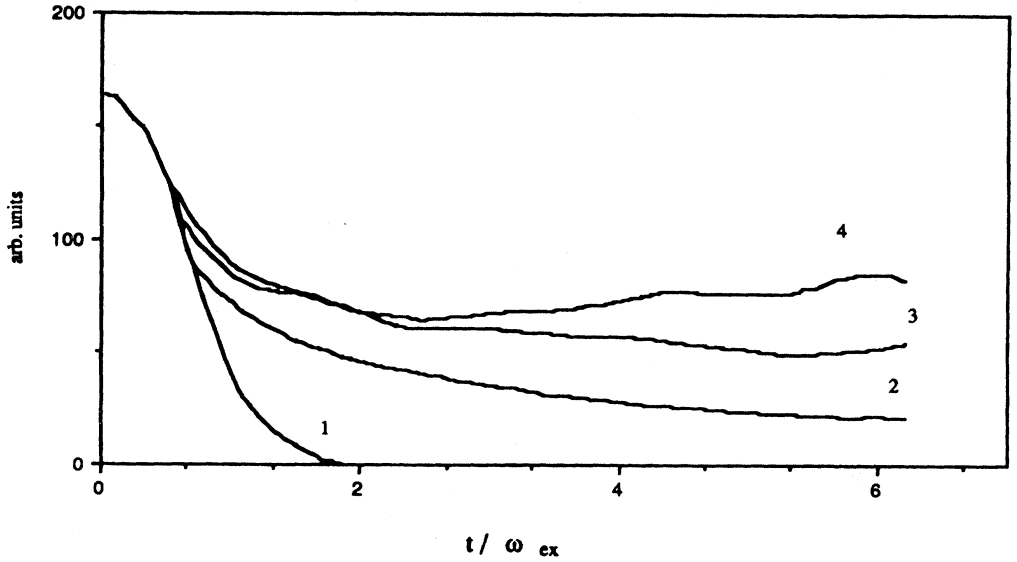

FIG. 10. Time evolution of spin correlation functions for finite magnetic chains: 1, Gaussian part; 2, diffusive part; 3, finite n=seven-spins chain; 4, finite n=five spins chain.

$$\tilde{f}(\omega)=G-n[{}_{\mathrm{ex}}\Pi D(x)]^{-1}+[2D(x)\omega]^{-1/2} . \quad (5)$$

G represents the contribution of $[g(t)-n^{-1}]$ at shorter times ($\sim\omega_{\mathrm{ex}}^{-1}$).

The combination of this model with Ref. 4 gives a qualitative' agreement with experimental results: the frequency variation with an "effective" diffusion coefficient enhanced by the doping, and the negatively increasing $P(x)$. We have to find the origin of the diffusion. Let us recall briefly the conditions in pure TMMC. We know that the total spin components S^z and S^+ commute with the Heisenberg Hamiltonian while S^z commutes with the secular intrachain dipolar interaction. Thus $f_j^z(\omega)$ and $f_j^+(\omega)$ can show a diffusive behavior provided that $\omega \gg \omega_c^{\alpha}$: the respective cutoff frequencies ω_c^z corresponding to the "longitudinal" electron relaxation rate, identified with T_{1e}^{-1} in TMMC, and ω_c^+ to the "transversal" rate, i.e., the ESR linewidth. For $\theta\sim 0°$, $\sum_i A_j$ is very small, owing to nearly perfect compensation of the A_j terms,[4] so the diffusive behavior of the functions $\tilde{f}_j^+(\omega)$ is only observed. At other orientations the diffusion is not observed because ω_c^z is itself frequency dependent.

In doped TMMC there are additional interactions: exchange or dipolar interactions between chain ends then can allow diffusion processes. However, it is highly doubtful that the observed diffusion is related to the behavior of $\sum_j B_j f_j^+(\omega_e)$ as in the pure case. The main reason is that it would imply extremely low values of $D(x)$: more than 10^3 smaller than the pure case value. As a result, the following condition required for probing the diffusion zone is not fulfilled: $\omega_e \ll t_D^{-1}\sim D(x)$. On the other hand the condition can be observed for ω_n, and we think that the diffusive behavior occurring near $\theta=0°$ in doped TMMC is indeed related to $\tilde{f}_j^z(\omega_n)$:

(i) Owing to the existence of impurities in the chains, the symmetry is broken and there is no more compensation of the A_j terms.

(ii) The cutoff frequency

$$\omega_c^z = T_{1e}^{-1}\sim 10^8 \text{ rad s}^{-1}$$

near $\theta=0°$, corresponding to a nuclear frequency $\nu_n=15$ MHz. In effect, T_{1n} appears to be frequency independent below this value. It results that $f_j^+(\omega_e)\ll\tilde{f}_j^z(\omega_n)$ so that

$$T_1^{-1}(x)\approx(\tfrac{2}{3}S(S+1)\sum_j A_j f_j^z(\omega_n) .$$

The averaged relaxation rate can be evaluated by considering, as in Ref. 4, the probability that a Mn^{2+} ion belongs to a chain of n spins and the resulting effect on the geometric terms. One obtains

$$T_1^{-1}=Q(x)+(\tfrac{2}{3})S(S+1)[2D(x)\omega_n]^{-1/2}A(x)$$

with

$$A(x)=\sum_j A_j(1-x)^{j+1} .$$

The value of $D(x)$ obtained from

$$[P(x)/P(x=0)]=(\omega_e/\omega_n)^{1/2}\left[A(x)\Big/\sum_j B_j\right]\times[D(x=0)/D(x)]^{1/2}$$

is given in Table I with other parameters. As in the TMMC-Cu, it is possible to interpret the average diffusion coefficient by means of a relation

$$[D(x)]^{-1}=(1-2x)[D(0)]^{-1}+2x(\tilde{D})^{-1} ,$$

$\tilde{D}$ being a "local" diffusion coefficient related to the Mn-

TABLE I. Experimental and theoretical parameters for the proton spin-lattice relaxation rates. $P(x)$ and $Q(x)$ are experimental parameters (Ref. 1) obtained from Fig. 9. $A(x)$ is an interaction parameter calculated for the impurity concentration x. $\alpha=\gamma_e\gamma_n\hbar$ where γ_e and γ_n are, respectively, the electron and nuclear gyromagnetic ratio. $D(x)$ (the diffusion coefficient) and $\tilde{D}$ (the "local" diffusion coefficient) are deduced from experiment.

x	$Q(x)$ (s^{-1})	$P(x)$ (10^6 $s^{-3/2}$)	$\alpha A(x)$ (10^{-6} Å^{-6})	$D(0)/D(x)$	$D(0)/\tilde{D}$
0	350	3.92	0.5	1	
0.02	−700	15	10.5	168	(3600)
0.09	−4700	61	32	300	1650
0.20	−12000	150	49.7	750	1865

Mn interaction between chain ends. One notes the good consistency of the $D/\tilde{D}$ values obtained in the two most doped samples. In fact, the rather high uncertainty comes from the lack of accuracy of the $A(x)$ value. The less doped sample contains semilong chains ($n \leq 10$) for which the spin dynamics model is not valid: The diffusion processes are established before the asymptotic value is reached.

The frequency term $Q(x)$ cannot be calculated easily. However, it can be seen from the relations (4) and (5) that it contains a negative part proportional to $[xD(x)]^{-1}$ which is strongly enhanced by the doping. Of course, the relaxation rate is not described in the whole range of frequencies by relation (1), since it would give unphysical results at high frequencies. The spectral density $f(\omega)$ is not diffusive at low frequencies (if ω is below the cutoff), but also at high frequencies, if ω is greater than, approximately, the spin-diffusion coefficient in frequency unit. As a result, one has not $T_1^{-1}\rightarrow Q$ when $\omega\rightarrow\infty$, and, of course, the T_1^{-1} value remains always positive and tends towards zero since $f(\omega\rightarrow\infty)\rightarrow 0$. In fact the spectral densities $f(\omega)$ tend towards zero as ω is increased. The model used and the resulting relations (4) and (5) are valid only for frequencies $\omega \ll t_D^{-1}$.

C. Analysis of the ESR results

The "dipolar" function $\phi(t)$ can be constructed like $g_j(t)$. For a finite chain of n spins ($n \leq 10$), $\phi(t)$ rapidly attains a constant value. The computer simulation on classical spins shows that

$$\phi(t\rightarrow\infty)/\phi(0)=C$$

is approximately equal to $n^{-1/2}$. For a sample with a concentration x of impurities we define a mean value $C(x)$. The correlation function is written as (the initial Gaussian decay being neglected)

$$\phi(t)=\phi(0)C(x)e^{-\omega_c t} \text{ for } 0\leq t\leq t_D ,$$

$$\phi(t)=\phi(0)C(x)(t_D/t)^{1/2}e^{-\omega_c t} \text{ for } t_D\leq t\leq\infty .$$

$\phi(0)$ is obtained from spin decoupling

$$\phi(0)=(\tfrac{8}{3}\zeta(6)S(S+1), \quad \zeta(x)=\sum_n n^{-x} .$$

Before a direct comparison between experiment and theory, let us focus on a specific point. It has been shown that the ESR spectrum is a function of the angle between the chain axis **c** and the oscillating field polarization: It is characterized by a line shift and an alteration of the shape and the amplitude of the line.[19] In our experiment the oscillating field is nearly perpendicular to the plane containing **c** and the static field ($\varphi=90°$), so the resulting line shift is negligible and the most visible effect appearing in the derivated line is a greater peak in the upper field side. The important shifts that are observed are related to the complex spectral densities $\tilde{\Phi}(\omega)$. The orientation $\theta=90°$ is of particular interest since it is known that, in this case, the spectrum can be described by means of generalized Bloch equations with two damping rates: $1/T_{2\text{ch}}$ along the chain axis, and $1/T_{2t}$ perpendicular to the chain:

$$1/T_{2t}\sim(\tfrac{9}{8})\omega_D^2[\tilde{\Phi}(\omega+\omega_z)+\tilde{\Phi}(\omega-\omega_z)] ,$$

$1/T_{2\text{ch}}$ being caused by the weaker interchain contribution. Low-frequency measurements have shown that[19]

$$1/T_{2\text{ch}}\sim 5\times 10^8 \text{ rad s}^{-1}$$

and

$$1/T_{2t}\sim 10^{10} \text{ rad s}^{-1}$$

in pure TMMC. If we apply the relation (7) of Ref. 19 to the linewidth measured at X-band in doped ($x=0.20$) TMMC we obtain

$$1/T_{2t}\sim 3.4\times 10^{10} \text{ rad s}^{-1}$$

($1/T_{2\text{ch}}$ has a negligible influence). Of course this calculation is not rigorous since the field dependence of the damping rate has been neglected, but it shows that the spectral density $\phi(0)$ is altered by the doping, but in a lesser extent than the two-spin $f(0)$. A cause is the enhancement of the cutoff frequency, varying approximately as the linewidth. An approximate value of the cutoff for $\theta=90°$ can be obtained by considering the spectrum in the relaxation configuration. In this case one can write $I_z\propto\text{Re}[\tilde{\Phi}(\omega-2\omega_z)]$. Let us suppose, for simplicity, that no diffusion occurs for $\phi(t)$ (i.e., $t_D\rightarrow\infty$). It follows

$$\omega_c\sim 3^{1/2}\gamma_e\Delta H_{pp}\sim 2.5\times 10^{10} \text{ rad s}^{-1} .$$

TABLE II. The $C(x)$ and t_D values necessary to compute the linewidths. The values of $C(x)$ should be compared to the values obtained from simulations on classical chain of n spins:[24] $C \approx 0.4$ for $n=5$ and $C \approx 0.25$ for $n=10$.

x (doping rate)	$C(x)$	$t_D(x)$ (in $\tilde{J}$ units)
0.02	0.15	24
0.09	0.3	30
0.20	0.5	55

From the $1/T_{2t}$ value previously calculated we deduce $C(x=0.20) \sim 0.35$.

Now we return to the model, taking into account a possible spin diffusion. To compute numerically the ESR spectra we calculate the transform of $\phi(t)$. Three parameters must be considered in order to fit the experimental and computed linewidths and shifts for the two configurations: the amplitude $C(x)$, the diffusive time t_D, and the cutoff frequency ω_c. In fact the ω_c value is locked to the linewidth: $\omega_c \sim \alpha \Delta H_{pp}$.

The $C(x)$ and $t_D(x)$ values chosen are given in Table II. For the resonance configuration the agreement is quite satisfactory for the linewidths and quantitatively gratifying for the line shift (Figs. 2 and 3). For the relaxation configuration it is merely passable. The lengthening of the spin-lattice relaxation time T_{1e} is related to the rapid decreasing of spectral densities $\tilde{\Phi}(\omega)$ at high frequencies resulting from the reduced diffusive part. It should be noted that, as for the nuclear relaxation, there is a broad range of T_{1e} in the sample. Furthermore, the method of measurement tends to favor the longer T_1 (the signal delivered by the modulation spectrum is a growing function of T_1) and a quantitative comparison with theory is not easy.

VI. CONCLUSION

We have reported in this publication ESR experiments on TMMC-doped samples. Two configurations of the oscillating field have been considered: the resonance and the relaxation ones. We have also measured the electron longitudinal relaxation rate using the modulation method. These experiments point out evidence of considerable effects both on the linewidths (enhancement) and on the electron spin-lattice rate (reduction). New NMR data dealing with high-frequency proton relaxation rates have also been reported. Besides the very strong shortening of the proton spin-lattice relaxation time caused by the doping, one notes a frequency dependence giving evidence of a spin diffusion of two-spin correlation functions, as in pure TMMC. Here, however, the longitudinal (in the field direction) spin fluctuations are involved, contrarily to the pure case. The diffusion occurs through the weak interactions between Mn ions across a Cd impurity. A correlation function model with delayed diffusion time has been proposed to account for the considerable effects observed in NMR and ESR. The ESR spectrum has been divided from a generalized memory-function formalism. The ESR linewidths and line shifts so calculated are in fairly good agreement with experiment. The diffusion time values t_D obtained from NMR and ESR appeared to be quite different. However, the behaviors of the two-spin function $g(t)$ and the dipolar function $\phi(t)$ cannot be compared in the diffusion regime because the decoupling procedure is not expected to be valid in this case. We note also that the enormous shift observed in the relaxation configuration remains to a large extent unexplained. A more realistic model of spin dynamics is thus needed.

ACKNOWLEDGMENTS

One of the authors (S.C.) wishes to thank Dr. J. P. Boucher and Dr. M. Nechtschein for their kind hospitality at the Centre d'Etudes Nucléaires de Grenoble where NMR measurements were performed. Institut d'Electronique Fondamentale is a laboratoire associé au Centre National de la Recherche Scientifique.

APPENDIX

For a linear chain of spins, the $a^{\mu\beta}$ terms occurring in relations (2) and (3) can be expressed as

$$a^{+-}=i(\omega+\omega_z)+B\{(1-3\cos^2\theta)^2\tilde{\Phi}(\omega+\omega_z)+\sin^2\theta\cos^2\theta[6\tilde{\Phi}(\omega)+4\tilde{\Phi}(\omega+2\omega_z)]+\sin^4\theta\Phi(\omega-\omega_z)\}\ ,$$

$$a^{-+}=i(\omega-\omega_z)+B\{(1-3\cos^2\theta)^2\tilde{\Phi}(\omega-\omega_z)+\sin^2\theta\cos^2\theta[6\tilde{\Phi}(\omega)+4\tilde{\Phi}(\omega-2\omega_z)]+\sin^4\theta\tilde{\Phi}(\omega+\omega_z)\}\ ,$$

$$a^{zz}=i\omega+B\{\sin^2\theta\cos^2\theta[\tilde{\Phi}(\omega+\omega_z)+\tilde{\Phi}(\omega-\omega_z)]+\sin^4\theta[\tilde{\Phi}(\omega+2\omega_z)+\tilde{\Phi}(\omega-2\omega_z)]\}\ ,$$

$$a^{2+}=Be^{2i\varphi}\{(1-3\cos^2\theta)\sin^2\theta[\tilde{\Phi}(\omega+\omega_z)+\tilde{\Phi}(\omega-\omega_z)]+6\sin^2\theta\cos^2\theta\tilde{\Phi}(\omega)\}\ ,$$

$$a^{-z}=Be^{-i\varphi}[2(1-3\cos^2\theta)\sin\theta\cos\theta y(\omega-\omega_z)-4\sin^3\theta\cos\theta\tilde{\Phi}(\omega-2\omega_z)-2\sin^3\theta\cos\theta\tilde{\Phi}(\omega+\omega_z)]\ ,$$

$$a^{z-}=Be^{-i\varphi}[(1-3\cos^2\theta)\sin\theta\cos\theta\tilde{\Phi}(\omega+\omega_z)-2\sin^3\theta\cos\tilde{\Phi}(\omega+2\omega_z)-\sin^3\theta\cos\tilde{\Phi}(\omega-\omega_z)]\ ,$$

$$a^{+-}(\omega_z)=a^{-+}(-\omega_z)\ ,$$

$$a^{z-}(\omega_z)=a^{-z}(-\omega_z)\ ,$$

with $B=(\frac{9}{16})\omega_D^2$ and $\omega_D=\hbar\gamma_e^2/c^3$ the dipolar frequency, c the smallest separation between ions in the chain, and γ the gyromagnetic ratio. The chain axis c is defined by spherical coordinates (θ,φ), the static magnetic field H_0 being directed along the z axis.

$\tilde{\Phi}(\omega)$ is the Laplace transform of the four-spin correlation function

$$\Phi(t)=e^{-\omega_c t}\sum_{ijkl}(i-j)^{-3}(k-l)^{-3}\langle S_i^+(t)S_j^+(t)S_j^-S_k^-\rangle/\langle S^+S^-\rangle \ ,$$

where the evolution of the spins ($S_i^{\pm}$ are the ladder operators at site i) is governed by exchange interaction only. The effect of the dipolar interaction is described in a phenomenological way by the cutoff frequency ω_c.

[1]J. P. Boucher, M. Ahmed, M. Nechtschein, M. Villa, G. Bonera, and F. Borsa, Phys. Rev. B **13**, 4098 (1976).
[2]P. M. Richards, Phys. Rev. B **10**, 805 (1974); **13**, 458 (1976); S. Clément, C. Dupas, J. P. Renard, and A. Cheikh-Rouhou, J. Phys. **43**, 767 (1982).
[3]S. Clément and Y. H. Tchao, C. R. Acad. Sci. **282B**, 165 (1976).
[4]S. Clément, T. V. Hiep, and J. P. Renard, Solid State Commun. **37**, 967 (1981).
[5]S. Clément, J. P. Renard, and G. Ablart, J. Magn. Res. **60**, 46 (1984).
[6]N. Shah, G. Kemmer, and J. S. Karra, Phys. Rev. B **27**, 5360 (1983).
[7]J. S. Karra and G. Kemmer, Phys. Rev. B **31**, 7430 (1985).
[8]B. Morosin and E. Graeber, Acta Crystallogr. **23**, 766 (1967).
[9]B. Morosin, Acta Crystallogr. **28**, 2303 (1972).
[10]H. Hervé and J. Pescia, C. R. Acad. Sci. **25**, 665 (1960).
[11]G. Ablart and J. Pescia, Phys. Rev. B **22**, 1150 (1980).
[12]J. Gourdon, B. Vigouroux, and J. Pescia, J. Phys. Lett. **45A**, 69 (1973).
[13]D. Bourdel, F. Ruiz, G. Ablart, J. Pescia, S. Clément, and J. P. Renard, Solid State Commun. **29**, 727 (1979).
[14]C. Dupas and J. P. Renard, Phys. Rev. B **18**, 401 (1978).
[15]G. L. McPherson, L. M. Henling, R. C. Koch, and H. F. Quarls, Phys. Rev. B **16**, 1893 (1977); Y. Tazuke, J. Phys. Soc. Jpn. **42**, 1617 (1977).
[16]A. Lagendijk and D. Schoemaker, Phys. Rev. B **16**, 47 (1977).
[17]E. Siegel, J. Ibrugger, and A. Lagendijk, J. Phys. C **15**, 4583 (1982).
[18]S. Clément, E. Bize, and J. P. Renard, Phys. Rev. Lett. **53**, 2508 (1984).
[19]E. Bize, S. Clément, and J. P. Renard, Phys. Rev. B (to be published).
[20]N. Bloembergen and S. Wang, Phys. Rev. **93**, 72 (1954).
[21]R. Kubo and K. Tomita, J. Phys. Soc. Jpn. **9**, 888 (1954).
[22]P. Beauvillain, S. Clement, and P. Veillet (unpublished).
[23]R. Zwanzig, J. Chem. Phys. **33**, 1338 (1960).
[24]T. V. Hiep, thèse de doctorat d'Etat, Université Paris XI (Orsay), 1982 (unpublished).